

## Mott Physics near the Insulator-To-Metal Transition in NdNiO<sub>3</sub>

M. K. Stewart,<sup>1,\*</sup> Jian Liu,<sup>2,3</sup> M. Kareev,<sup>2</sup> J. Chakhalian,<sup>2</sup> and D. N. Basov<sup>1</sup>

<sup>1</sup>Department of Physics, University of California-San Diego, La Jolla, California 92093, USA

<sup>2</sup>Department of Physics, University of Arkansas, Fayetteville, Arkansas 72701, USA

<sup>3</sup>Advanced Light Source, Lawrence Berkeley National Laboratory, Berkeley, California 94720, USA

(Received 18 April 2011; published 17 October 2011)

An optical study of NdNiO<sub>3</sub> ultrathin films with insulating and metallic ground states reveals new aspects of the insulator-to-metal transition that point to Mott physics as the driving force. In contrast with the behavior of charge-ordered systems, we find that the emergence of the Drude resonance across the transition is linked to a spectral weight transfer over an energy range of the order of the Coulomb repulsion  $U$ , as the energy gap is filled with states instead of closing continuously.

DOI: 10.1103/PhysRevLett.107.176401

PACS numbers: 71.27.+a, 72.80.Ga, 78.20.-e, 78.30.-j

The rare earth nickelates have been of interest to researchers in part due to the strong connection between their crystal structure and electronic and magnetic properties [1,2]. With the exception of LaNiO<sub>3</sub> (LNO), the members of the RNiO<sub>3</sub> series ( $R$  = rare earth) undergo an insulator-to-metal transition (IMT) at a temperature  $T_{\text{IMT}}$ , which can be controlled by the radius of  $R$  [3], applied hydrostatic pressure [4,5] or epitaxial strain [6]. It is believed from resonant x-ray diffraction [7], transport [8] and electron diffraction [9] studies that a structural phase transition resulting in charge ordering is responsible for the IMT. Furthermore, it has been suggested that the ground state of the nickelates can in fact be better understood as a band insulator rather than a Mott-Hubbard system [10]. However, given the recent optical studies of LNO that have shown unusually strong electronic correlations and a spectral weight (SW) transfer consistent with Mott physics [11,12], it is possible that the current understanding of the IMT in nickelates based solely on charge ordering is incomplete.

In this Letter we present an optical study of newly available ultrathin films of NdNiO<sub>3</sub> (NNO) in which the IMT can be quenched by applying compressive strain [13]. In the bulk, NNO undergoes a transition from an antiferromagnetic insulator [14] to a paramagnetic metal at  $\sim 200$  K [3], accompanied by a structural transition [15]. While detailed optical studies of NNO ceramics exist [16], no such characterization of NNO single crystals or epitaxial ultrathin films has been reported. The ability to grow and study high quality samples with tunable properties allows one to thoroughly investigate the processes involved in the IMT. A SW analysis of our data reveals key signatures of Mott-Hubbard physics, providing strong evidence that electronic correlations play a major role in achieving the insulating phase in NNO.

Epitaxial NNO films were grown on LaAlO<sub>3</sub> (LAO) and SrTiO<sub>3</sub> (STO) substrates by pulsed laser deposition with *in situ* monitoring by reflection high energy electron diffraction. Single crystal LAO (001) and STO (001)

substrates provide  $-0.3\%$  and  $+2.6\%$  lattice mismatch, respectively. The films are 30 u.c. thick with  $c$ -axis parameters of 3.84 Å on LAO and 3.75 Å on STO. Growth conditions and sample characterization details can be found in Ref. [13].

The optical characterization of the films and bare substrates was carried out using variable angle spectroscopic ellipsometry (VASE) in the range from 60 meV to 6 eV and near normal incidence reflectance in the range from 10 to 80 meV. Ellipsometric measurements were performed with two commercial Woollam ellipsometers equipped with home-built UHV cryogenic chambers. Reflectance of the samples was measured in a Michelson interferometer (Bruker 66vs) relative to a gold mirror and then normalized by the reflectance of the gold coated sample [17]. In order to obtain the optical constants from the raw reflectance and ellipsometry data, a model was created using multiple Kramers-Kronig consistent oscillators to parametrize the complex dielectric function of the sample [18]. The parameters in the model were then fitted to the experimental data using regression analysis. We first obtained the optical constants of the bare substrates. These were then used in a two-layer film-substrate model, employed to extract the dielectric functions of the films alone. Since LAO and STO have several far-IR phonons with strong temperature dependence, the substrates were measured and modeled at all the same temperatures as the films. This allowed us to use the appropriate temperature for the substrate layer, thus ensuring that the temperature dependence observed in the extracted optical conductivity is indeed caused by the NNO films [19].

We first consider the real part of the optical conductivity  $\sigma_1(\omega)$  given by  $\sigma(\omega) = \frac{i\omega[1-\epsilon(\omega)]}{4\pi}$ , where  $\epsilon(\omega)$  is the complex dielectric function. The room temperature  $\sigma_1(\omega)$  for the NNO films on LAO and on STO is shown in Fig. 1. Below 2 eV the two spectra exhibit the same gross features: a Drude peak and two interband transitions labeled  $A$  and  $B$  in Fig. 1. The Drude resonance is stronger for the film on LAO. Based on bulk band structure

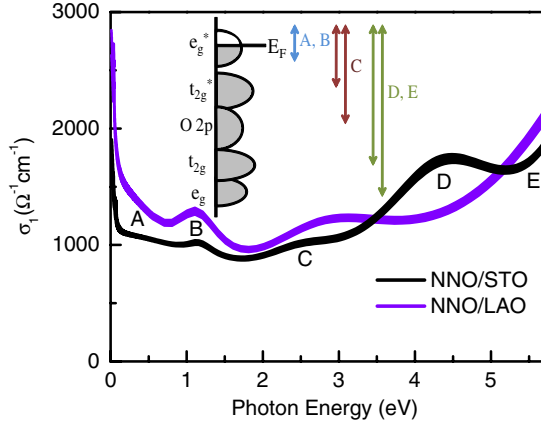


FIG. 1 (color online). Real part of the optical conductivity at 298 K for the NNO films on LAO and STO. The error bars are represented by the thickness of the curves. Inset: sketch of the NNO DOS based on Refs. [20,21].

calculations showing a  $t_{2g}^6 e_g^1$  electronic configuration [20,21], we suggest that features *A* and *B* are due to transitions between the occupied and unoccupied antibonding  $e_g^*$  orbitals (see inset in Fig. 1). Above 2 eV, more marked differences between the two spectra are evident. Feature *C* is broader and centered at higher frequency for the film on LAO and a peak at 4.5 eV (feature *D*) is only evident for the film on STO. Feature *C* can be assigned to transitions from the  $t_{2g}^*$  and the nonbonding O 2p to the  $e_g^*$  orbitals. Finally, *D* and *E* could be the result of excitations from the bonding  $t_{2g}$  and  $e_g$  levels to  $e_g^*$ . Transitions to the empty Nd 4f and 5d states could also contribute to the higher energy features *D* and *E*, but band structure calculations with density of states (DOS) including these orbitals were not available. We note that these assignments are based on calculations performed for bulk NNO and not for strained films.

The optical conductivity of the NNO film on STO at various temperatures can be seen in Fig. 2. At low temperature the Drude peak disappears as the system enters the charge-ordered insulating state. The SW of feature *A* rapidly decreases and a new peak emerges at 0.65 eV (*A'* in Fig. 2). This transfer of SW from the Drude resonance to a finite energy peak is typical of charge-ordered systems in the regime of weak electron-lattice coupling [22,23]. However, feature *A'*, which is likely due to transitions between the  $e_g^*$  states that are gapped in the insulating state, only accounts for part of the lost Drude SW. We must therefore consider feature *D*, which shows a temperature dependence opposite to that of the Drude response: Its SW decreases as the temperature is raised from 20 K to 200 K and then increases when warmed up further. Thus, this resonance is clearly involved in the SW transfer that leads to the opening of the correlated gap, as evidenced by the SW analysis presented below.

Figure 3 shows  $\sigma_1(\omega)$  for the NNO film on LAO. In contrast with the film on STO (Fig. 2) and bulk NNO [16],

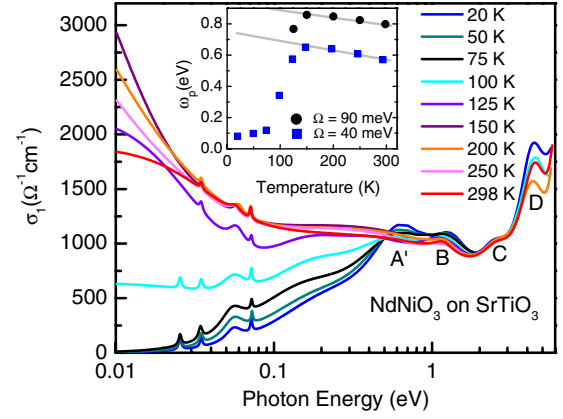


FIG. 2 (color online). Real part of the complex conductivity for the NNO film on STO across the IMT. Inset:  $\omega_p$  obtained from Eq. (1) with  $\Omega = 90$  meV and plasma frequency obtained with  $\Omega = 40$  meV. The gray lines are guides to the eye.

the Drude resonance remains prominent at 20 K and its magnitude increases. The peak *A'* that arises at low temperature for the film on STO between features *A* and *B* as a result of the IMT is not seen. This is consistent with x-ray absorption data showing a charge-ordered ground state for the film on STO but not for the film on LAO [13]. Finally, we observe an unusual transfer of SW from feature *C* to the Drude peak, which we discuss in detail below.

To quantitatively study the temperature dependence of the Drude resonance in the metallic phase we consider the plasma frequency  $\omega_p$  given by

$$\frac{\omega_p^2}{8} = \int_0^\Omega \sigma_1(\omega) d\omega = \frac{4\pi n e^2}{m^*}. \quad (1)$$

Here  $n$  is the density of free carriers,  $m^*$  is their renormalized mass, and  $\Omega$  is the cutoff chosen to include only the

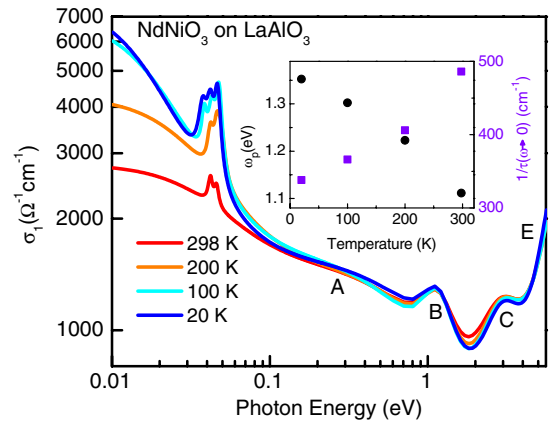


FIG. 3 (color online). Real part of the optical conductivity for the NNO film on LAO at various temperatures. The Drude resonance remains prominent at all temperatures and no IMT is observed. Inset:  $\omega_p$  and  $1/\tau$  obtained from Eqs. (1) and (2).

coherent contribution to  $\sigma_1(\omega)$ . In conventional metals the free carrier SW is unaltered with temperature and the entire temperature dependence of the Drude absorption is due to a decrease in the scattering rate  $1/\tau$ . Correlated metals, on the other hand, often exhibit an exotic temperature dependence of  $\omega_p$  [24]. In the normal state of high- $T_c$  cuprates, for instance, a  $\sim 2\%$  enhancement in  $\omega_p$  has been measured that can not be explained by the Sommerfeld model [25]. More recently, a low temperature increase in the Drude SW of unprecedented magnitude was observed in LaNiO<sub>3</sub> (LNO) [12].

For the film on LAO  $\omega_p$  was obtained using  $\Omega = 125$  meV, before the onset of feature A. Additionally,  $1/\tau$  was obtained from the extended Drude analysis using

$$\frac{1}{\tau(\omega)} = -\frac{\omega_p^2}{\omega} \text{Im}\left(\frac{1}{\tilde{\varepsilon}(\omega) - \varepsilon_\infty}\right). \quad (2)$$

$\omega_p$  and  $1/\tau(\omega \rightarrow 0)$  are plotted in the inset in Fig. 3. Similar to the behavior of LNO [12],  $1/\tau$  decreases at low temperature, but not enough to account for the change in dc resistivity [13]. The enhancement in  $\omega_p$  from 1.1 eV at 298 K to 1.35 eV at 20 K must also be taken into account, signaling that additional states are being populated at the Fermi energy. For the film on STO we used  $\Omega = 90$  meV, the minimum in  $\sigma_1(\omega)$  at 125 K between the Drude peak and the first interband transition A. A similar behavior to that of the film on LAO is observed at  $T > T_{\text{IMT}}$ . We find that  $\omega_p$  increases with decreasing temperature down to 150 K (see inset in Fig. 2). The inset in Fig. 2 also shows  $\omega_p$  integrated up to 40 meV, roughly the size of the insulating gap. As expected, the low frequency SW is close zero at low temperature and then increases rapidly as  $T_{\text{IMT}}$  is approached.

While both samples exhibit a low temperature enhancement of  $\omega_p$  in the metallic phase, the origin of this effect is not the same. To understand this better we consider the ratio of  $\sigma_1(\omega)$  at low temperature and at 298 K shown in the insets in Fig. 4. For the film on LAO there is a low temperature decrease in  $\sigma_1(\omega)$  between 1.5 and 4 eV and a transfer of SW from feature C to the Drude resonance. This can also be seen by studying  $\text{SW}(\Omega)$ , which represents the effective number of carriers contributing to absorption below the cutoff frequency  $\Omega$  and is given by [26]

$$\text{SW}(\Omega) = \int_0^\Omega \sigma_1(\omega) d\omega. \quad (3)$$

Figure 4(a) shows the ratio of the SW at various temperatures and that at 298 K for the film on LAO. For  $\Omega = 1.2$  eV, which includes the contributions from interband transitions A and B, the SW is 10% higher at 20 K than at 298 K.  $\text{SW}(\Omega = 4$  eV), on the other hand, is the same at all temperatures, confirming the transfer of SW from feature C to the Drude resonance.

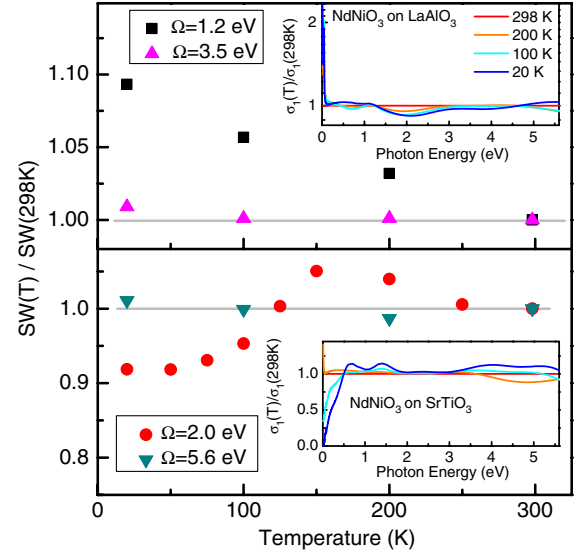


FIG. 4 (color online). Ratio of the SW Eq. (3) at low temperature and at 298 K obtained with various frequency cutoffs  $\Omega$  for the films on LAO (a) and on STO (b). The gray lines are guides to the eye. Insets: Ratio of  $\sigma_1(\omega)$  at low temperature and at 298 K.

For the film on STO,  $\sigma_1(\omega)$  is enhanced above 3.5 eV at 200 K and then suppressed in the insulating state.  $\text{SW}(\Omega = 2$  eV), which includes features A and B, increases down to 150 K and then decreases in the insulating state [Fig. 4(b)]. With  $\Omega = 5.6$  eV we find that the SW is nearly the same at all the measured temperatures. This behavior is drastically different from systems where the IMT is caused by charge- and/or spin- ordering. These latter effects lead to the opening of an energy gap with a transfer of the free carrier SW to resonances immediately above it [23]. In Fe<sub>3</sub>O<sub>4</sub>, for example, the redistribution of SW is restricted to 10 times the size of the energy gap  $\Delta$  [22], instead of up to  $30\Delta$  as we observe for NNO. Our data are also in contrast with spin density wave systems, such as Cd<sub>2</sub>Os<sub>2</sub>O<sub>7</sub> [27], in which the gap closes continuously. Instead, like in other Mott systems [28], Fig. 2 shows that  $\sigma_1(\omega)$  increases gradually in the gap region as it is filled with states. Contrary to the conventional understanding, these two observations indicate that charge ordering, if present, is not the driving force for the IMT in NNO.

Our data suggest that the different ground states observed for the two films are linked to the contrast seen in the high energy  $\sigma_1(\omega)$ , namely, features C and D (Fig. 1). While we have tentatively attributed these peaks to different interband transitions (Fig. 1 inset), *ab initio* calculations taking into account the modified crystal structure of the strained films are necessary to be sure of this assignment. Irrespective of this uncertainty, our observations are consistent with the Mott-Hubbard picture for a strongly correlated metal and a Mott insulator. When a conducting state is initiated in a Mott-Hubbard system either by temperature or doping, the coherent contribution to  $\sigma_1(\omega)$

increases at low temperature as SW is transferred from the Hubbard band to the quasiparticle peak. This phenomenon occurs on the energy scale of  $U/2$ , where  $U$  is the on-site Coulomb repulsion. In the insulating state, on the other hand, the transitions related to the Hubbard bands will occur at energies on the order of  $U$  since there is no quasiparticle peak [29]. Similarly, our data show that the energy scale involved in the SW transfer for the NNO film on STO ( $\sim 5.6$  eV) is roughly twice as large as the one for the film on LAO ( $\sim 3$  eV) and suggest a range of  $U$  that is in reasonable agreement with  $U = 7$  eV reported previously [30]. We therefore propose that Mott physics plays an important role in the IMT of NNO, in contrast with the claims of Ref. [10] that the insulating state in the nickelates can be better described by a more conventional band picture.

While the optical data obtained for the film on LAO are very different from the film on STO and even bulk NNO, the spectra are surprisingly similar to those of LNO [12]. Not only does the sample remain metallic at all temperatures but the transfer of SW from feature  $C$  to the Drude resonance over the energy range of  $U/2$  and the dramatic increase in  $\omega_p$  are almost identical to the temperature dependence of LNO. The interband transitions in Fig. 3 are remarkably similar to those observed in ultrathin films of LNO on LAO as well.

Even though applying hydrostatic pressure can cause a suppression of  $T_{\text{IMT}}$  due to an increase in the bandwidth, over 40 kbar would be required to fully quench the IMT [31], much more than can be achieved with the  $-0.3\%$  of epitaxial strain present in our films. We therefore propose that the stabilization of the metallic phase in the NNO film on LAO can not be understood in terms of a change in bandwidth and the effects of heteroepitaxial strain must be considered. Previous work on ultrathin films of LNO has shown that tensile and compressive strain result in different crystal structures for the films [32,33]. Compressive strain is accommodated by Ni-O bond bending and stretching, resulting in a distortion of the  $\text{NiO}_6$  octahedra and a reduced symmetry of the atomic structure relative to bulk LNO. In contrast, samples under tensile strain show a pronounced pattern of octahedral rotations with an additional “breathing” mode of the  $\text{NiO}_6$  network. This latter effect induces a Ni-O bond length disproportionation resulting in two inequivalent Ni sites [33].

This link between bi-axial strain and  $\text{NiO}_6$  structure could be responsible for the quenching of the IMT. Assuming a similar effect to that observed in LNO, the breathing distortion associated with deterrances in orbital polarization and ligand hole density distribution would be active for the film on STO but not for the film on LAO, thus precluding the charge-ordered ground state in the latter and stabilizing the unusual metallic phase. Orbital reflectometry experiments that can detect small variations in the orbital occupation [34] would therefore be helpful in

understanding the striking strain dependence we observed in the optical properties of NNO.

The discussion in the previous paragraph and the SW analysis presented above suggest that charge-ordering and Mott physics work together to produce the insulating state in NNO. We observe a transfer of SW from the Drude resonance to the peaks immediately above the insulating gap, typical of charge-ordering systems. However, we also find unambiguous evidence that the energy scales of the order of  $U$  are intimately involved in both the IMT and the charge dynamics of the metallic state. The simple band picture based solely on charge-ordering [10] fails to account for the salient spectral properties of nickelates presented in this letter and in Ref. [12] and Mott physics must therefore be taken into account to fully describe this correlated system.

Work at UCSD is supported by DOE-BES. J.C. was supported by DOD-ARO under the grant No. 0402-17291 and NSF grant No. DMR-0747808.

---

\*mstewart@physics.ucsd.edu

- [1] M. L. Medarde, *J. Phys. Condens. Matter* **9**, 1679 (1997).
- [2] G. Catalan, *Phase Transit.* **81**, 729 (2008).
- [3] J. B. Torrance *et al.*, *Phys. Rev. B* **45**, 8209 (1992).
- [4] P. C. Canfield *et al.*, *Phys. Rev. B* **47**, 12 357 (1993).
- [5] X. Obradors *et al.*, *Phys. Rev. B* **47**, 12 353 (1993).
- [6] A. Tiwari, C. Jin, and J. Narayan, *Appl. Phys. Lett.* **80**, 4039 (2002).
- [7] V. Scagnoli *et al.*, *Phys. Rev. B* **72**, 155111 (2005).
- [8] J. S. Zhou *et al.*, *Phys. Rev. B* **61**, 4401 (2000).
- [9] M. Zaghrioui *et al.*, *Phys. Rev. B* **64**, 081102 (2001).
- [10] I. Mazin *et al.*, *Phys. Rev. Lett.* **98**, 176406 (2007).
- [11] D. G. Ouellette *et al.*, *Phys. Rev. B* **82**, 165112 (2010).
- [12] M. K. Stewart *et al.*, *Phys. Rev. B* **83**, 075125 (2011).
- [13] J. Liu *et al.*, *Appl. Phys. Lett.* **96**, 233110 (2010).
- [14] J. L. Garcia-Munoz, J. Rodriguez-Carvajal, and P. Lacorre, *Phys. Rev. B* **50**, 978 (1994).
- [15] J. L. Garcia-Munoz *et al.*, *Phys. Rev. B* **46**, 4414 (1992).
- [16] T. Katsufuji *et al.*, *Phys. Rev. B* **51**, 4830 (1995).
- [17] C. C. Homes *et al.*, *Appl. Opt.* **32**, 2976 (1993).
- [18] A. B. Kuzmenko, *Rev. Sci. Instrum.* **76**, 083108 (2005).
- [19] See Supplemental Material at <http://link.aps.org/supplemental/10.1103/PhysRevLett.107.176401> for additional details about ellipsometric measurements and analysis.
- [20] D. D. Sarma, N. Shanthi, and P. Mahadevan, *J. Phys. Condens. Matter* **6**, 10467 (1994).
- [21] S. Yamamoto and T. Fujiwara, *J. Phys. Soc. Jpn.* **71**, 1226 (2002).
- [22] S. K. Park, T. Ishikawa, and Y. Tokura, *Phys. Rev. B* **58**, 3717 (1998).
- [23] S. Ciuchi and S. Fratini, *Phys. Rev. B* **77**, 205127 (2008).
- [24] L. Benfatto, J. P. Carbotte, and F. Marsiglio, *Phys. Rev. B* **74**, 155115 (2006).
- [25] M. Ortolani, P. Calvani, and S. Lupi, *Phys. Rev. Lett.* **94**, 067002 (2005).
- [26] D. N. Basov *et al.*, *Rev. Mod. Phys.* **83**, 471 (2011).

- 
- [27] W. J. Padilla, D. Mandrus, and D. N. Basov, *Phys. Rev. B* **66**, 035120 (2002).
- [28] M. M. Qazilbash *et al.*, *Phys. Rev. B* **79**, 075107 (2009).
- [29] M. J. Rozenberg *et al.*, *Phys. Rev. Lett.* **75**, 105 (1995).
- [30] S. M. Butorin *et al.*, *Solid State Commun.* **135**, 716 (2005).
- [31] J. S. Zhou, J. B. Goodenough, and B. Dabrowski, *Phys. Rev. Lett.* **95**, 127204 (2005).
- [32] S. J. May *et al.*, *Phys. Rev. B* **82**, 014110 (2010).
- [33] J. Chakhalian *et al.*, *Phys. Rev. Lett.* **107**, 116805 (2011).
- [34] E. Benckiser *et al.*, *Nature Mater.* **10**, 189 (2011).